Theoretical Model Studies for Surface-Molecule Interacting Systems

HIROSHI NAKATSUJI

Department of Synthetic Chemistry, Faculty of Engineering, Kyoto University, Kyoto 606, Japan and Institute for Fundamental Chemistry, Nishi-Hiraki-cho, Kyoto 606, Japan

Abstract

Surface-molecule interactions and reactions are important elementary steps of catalytic reactions. Since they involve interactions between infinite and finite systems, modelings are necessary for theoretical investigations of catalytic reactions on a surface. The cluster model (CM) is most frequently used for quantum chemical calculations but neglects the effect of the bulk solid. For including such effect, (1) embedding the cluster onto a surface (actually into a larger cluster) is a method proposed by Grimley and Pisani, and (2) dipping the adcluster (admolecule + cluster) onto the electron bath of the solid and letting the system be at equilibrium for electron and spin exchanges is another model proposed by Nakatsuji. We show some applications of the embedding cluster model (ECM) and the dipped adcluster model (DAM). We will also report in the lecture on the study of the photochemical decomposition reaction of MnO_4^- into $MnO_2^- + O_2$. © 1992 John Wiley & Sons, Inc.

Introduction

Chemistry and physics of surface-molecule interaction and reaction systems are of much interest from both purely scientific and industrial standpoints. Since these interactions involve finite and infinite systems, modelings are necessary for theoretical investigations of these systems. Since the results of the investigations are largely dependent upon the nature and the quality of the model adopted, we have to carefully examine the models for surface-molecule interactions and reactions.

Electron correlations are very important since we are mostly interested in the system involving transition metals. Since surface has many dangling bonds, it usually has several lower excited states and further the catalytically active state is not necessarily the ground state, so that our theory should be able to deal with both ground and excited states in a same accuracy. Moreover, electron transfer is sometimes of crucial importance for surface electronic processes and therefore should be described accurately.

Cluster model (CM) has been most frequently used by quantum chemists for investigating chemisorptions and catalytic reactions on metal and semiconductor surfaces. It also has a direct implication in the field of cluster chemistry growing up very rapidly in recent years. However, as a model of surface reactions, this model has a defect that it neglects the effect of bulk metal. For including such effect, Grimley, Pisani, and others proposed the embedded cluster model [1–3] and Nakatsuji the dipped adcluster model [4,5].

International Journal of Quantum Chemistry: Quantum Chemistry Symposium 26, 725–736 (1992)

CCC 0020-7608/92/010715-12

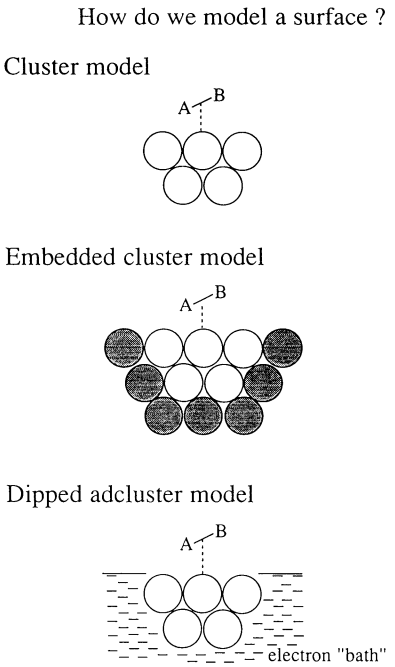

Figure 1. Conceptual sketch of the cluster model (CM), embedded cluster model (ECM), and dipped adcluster model (DAM).

Figure 1 is a sketch of the concepts of the embedded cluster model (ECM) and the dipped adcluster model (DAM) in comparison with the CM. We define the combined system of admolecule plus cluster in the CM as *adcluster*. Then, the CM is a free adcluster model. In the ECM, the cluster part of the adcluster is "embedded" onto the shaded cluster of atoms which are thought to represent the bulk. The direct interaction between the admolecule and the shaded part is neglected but its effect is taken into account effectively, using the Green's function formalism, in the calculation of the adcluster. On the other hand in the DAM, the adcluster is dipped onto the electron bath of the solid and is let to be in equilibrium for the electron exchange between the adcluster and the solid. This equilibrium is governed by the chemical potentials of the adcluster and the solid.

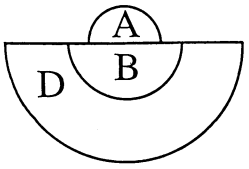

Figure 2. Schematic representation of the embedded cluster model. *A* is the adsorbate, *B* the cluster, and *D* represents the solid.

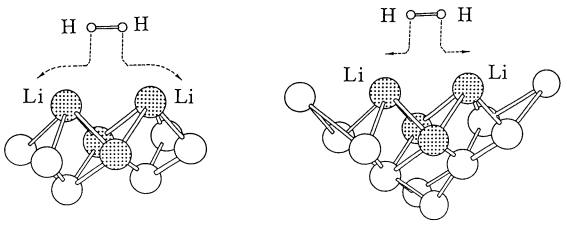

Figure 3. Li_{10} and Li_{14} clusters interacting with H_2, and Li_4 embedded onto Li_6 and L_{10} and interacting with H_2.

In this lecture, a brief account of our studies on the ECM and the DAM is given. More details will be published somewhere in the literature [5–9].

We also give in this lecture some results of the theoretical study for the photochemical decomposition reaction of permanganate ion [10,11].

Embedded Cluster Model Applied to H_2 Chemisorption on a Lithium Surface

We use here the moderately large embedded cluster (MLEC) model of Pisani, Ravenek, and others [2,3]. Figure 2 illustrates the definition of the model. A is an adsorbate, B is the cluster directly interacting with A, and D represents the solid.

In the closed-shell Hartree–Fock–Roothaan approximation,

$$F\,C = S\,C\,\varepsilon \tag{1}$$

the Green's function G and the matrix Q are defined by

$$Q(z)G(z) = 1 \tag{2}$$

$$Q(z) = zS - F \tag{3}$$

where S and F are, respectively, the overlap and Fock matrices. The Green's function G is further written as

$$G(z) = (zS - F)^{-1} \tag{4}$$

$$G_{\lambda\sigma}(z) = \sum_i \frac{C_{\lambda i} C_{\sigma i}}{z - \varepsilon_i} \tag{5}$$

where λ and σ stand for the basis in the LCAO approximation and $C_{\lambda i}$ is the MO coefficient of the orbital φ_i with the orbital energy ε_i. The essential steps of the ECM may be summarized as follows.

(1) Neglect the direct interaction between A and D

$$\begin{pmatrix} Q_{AA} & Q_{AB} & 0 \\ Q_{BA} & Q_{BB} & Q_{BD} \\ 0 & Q_{DB} & Q_{DD} \end{pmatrix} \begin{pmatrix} G_{AA} & G_{AB} & 0 \\ G_{BA} & G_{BB} & G_{BD} \\ 0 & G_{DB} & G_{DD} \end{pmatrix} = \begin{pmatrix} 1 & 0 & 0 \\ 0 & 1 & 0 \\ 0 & 0 & 1 \end{pmatrix} \tag{6}$$

(2) Calculate the free $B + D$ system without A

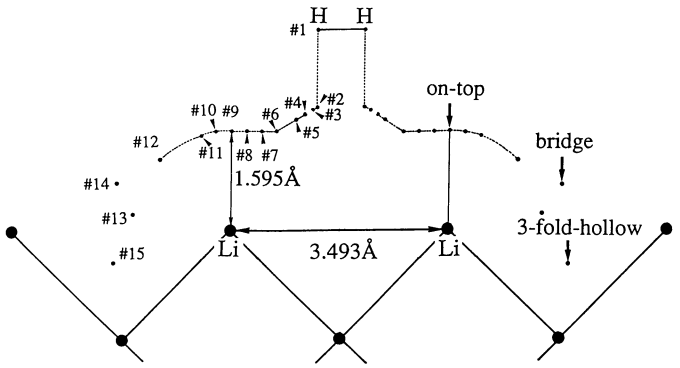

Figure 4. Reaction path for the H_2 adsorption on a Li surface. This reaction path keeps the C_{2V} symmetry and is the same for all of the five different cluster and embedded cluster calculations except that some Li atoms are missing in some models. Points 13, 14, and 15 are the most stable structures for the Li_4H_2, $Li_{14}H_2$, and $Li_{10}H_2$ clusters, respectively.

$$\begin{pmatrix} Q^f_{BB} & Q^f_{BD} \\ Q^f_{DB} & Q^f_{DD} \end{pmatrix}\begin{pmatrix} G^f_{BB} & G^f_{BD} \\ G^f_{DB} & G^f_{DD} \end{pmatrix} = \begin{pmatrix} 1 & 0 \\ 0 & 1 \end{pmatrix} \tag{7}$$

(3) Calculate only the $A + B$ system using the equation derived from Eq. (6) and approximate the interaction between B and D to be a constant which is given from the second step above.

$$\begin{pmatrix} Q_{AA} & Q_{AB} \\ Q_{BA} & Q_{BB} \end{pmatrix}\begin{pmatrix} G_{AA} & G_{AB} \\ G_{BA} & G_{BB} \end{pmatrix} = \begin{pmatrix} 1 & 0 \\ 0 & 1 - Q^f_{BD}G^f_{DB} \end{pmatrix} \tag{8}$$

We have adopted basically the calculational scheme given by Ravenek and Geurts, but added some modifications for improving convergence in the Green function calculation. Details are described elsewhere [6].

We have applied the embedded cluster model to an H_2 adsorption on a Li(100) surface. The calculated model systems are as follows:

(1) Li_{14} cluster interacting with H_2
(2) Li_{10} cluster interacting with H_2
(3) Li_4 cluster interacting with H_2
(4) Li_4 embedded onto Li_{10} interacting with H_2
(5) Li_4 embedded onto Li_6 interacting with H_2

Figure 3 illustrates the systems. The Li clusters are taken out from the Li(100) surface with the lattice constant fixed at 3.52 Å. The shaded Li_4 is the smallest cluster in the CM or the embedded cluster in the ECM. The gaussian basis is double-zeta (31) set for hydrogen and STO 3G plus diffuse s function ($\zeta = 0.076$) for lithium.

The assumed reaction pathway is displayed in Figure 4. The ECM is applicable only to the region from position 1 to position 10, since there the direct interaction between H_2 and the region D may be neglected. In this region the ECM calculations for the systems (4) and (5) above should simulate respectively the full-cluster cal-

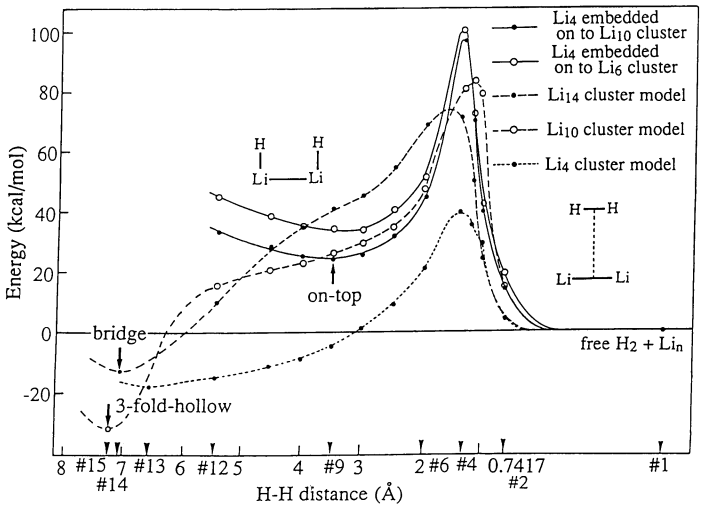

Figure 5. Potential curves for the H_2 adsorption on lithium.

culations for (1) and (2). As a cluster model calculation, we further perform calculations up to the positions 13 to 15.

Figure 5 shows the potential curves obtained by the CM and ECM. The minimum geometries and the corresponding energies are summarized in Table I. The following results may be deduced.

(1) Embedding the Li_4 cluster onto the larger cluster, the curve for the Li_4 cluster model is shifted up to those for the Li_4 embedded cluster models. This is reasonable in comparison with the curves obtained by the full-cluster model calculations.

(2) The value and the position of the barrier calculated by the CM is dependent on the cluster size, but those of the ECM is less dependent on the size of the region D. The barrier of the ECM is higher than that of the full cluster model, since the approximation of the fixed electronic effect of D on B can not fully describe the relaxation of the system.

TABLE I. Adsorption site, adsorption barrier, adsorption energy, and atomic population on H at the most stable adsorption geometry calculated by the cluster and embedded cluster models.

Cluster	Adsorption site	Adsorption barrier (kcal/mol)	Adsorption energy (kcal/mol)	Atomic population on H
Li_4 cluster	on-top	40.0	18.9	1.25
Li_{10} cluster	3-fold-hollow	84.8	31.2	1.23
Li_{14} cluster	bridge	72.3	14.2	1.22
Li_4 embedded onto Li_{10}	on-top	98.2	−24.7	1.29
Li_4 embedded onto Li_6	on-top	100.8	−34.9	1.28

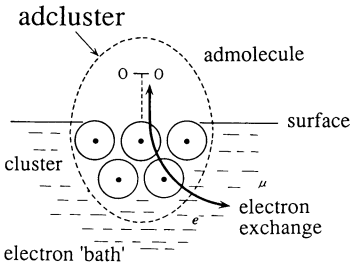

Figure 6. Illustration of the concept of the dipped adcluster model.

(3) The ECM gives a minimum at the on-top geometry, though it is less stable than the separated system. The corresponding full cluster model does not have such a minimum. This minimum may be artificial because the present ECM is too small for the regions of the points 9 to 12; the direct interaction between H_2 and the *D* region is not negligible there.

(4) In the CM calculations, the most stable geometries are the bridge site (position 14) for Li_{14}, the three-fold-hollow site (position 15) for Li_{10}, and the on-top site (position 13) for Li_4. The stabilization energies are summarized in Table I.

(5) The atomic charges of the adsorbed hydrogens are given in Table I and are between −0.2 and −0.3.

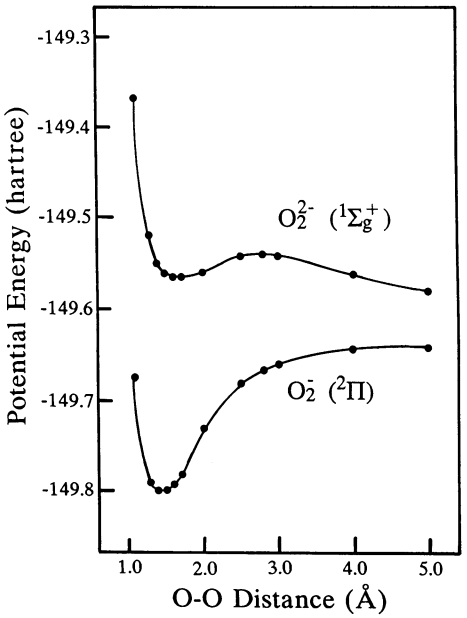

Figure 7. Potential energy curves for the ground states of dioxygen anion species, O_2^- and O_2^{2-}, calculated by the SAC/SAC-CI method.

The criticism of the present result is rather difficult. If the results of the embedded cluster model should reproduce those of the full-cluster model, the results shown in Figure 9 are by no means favorable to the embedded cluster model. On the other hand, if the D region of the embedded cluster model should be considered as representing a boundary of the bulk metal instead of an outer part of the larger cluster, the present result shown in Figure 9 is difficult to evaluate since there are no experimental estimations on the potential surface for the dissociative adsorption of H_2 on a Li surface, especially between #1 and #9.

For doing ECM calculations, we have to calculate the $B + D$ cluster, which is Li_{10} or Li_{14} in the present calculations. For studying catalytic activity of a metal surface, we have to deal with transition metals, and doing *ab initio* calculations for even this size of cluster is still a hard job. Further, accounts of electron correlations are very important for dealing with such systems. Therefore, satisfactory applications of the ECM to transition metal surfaces are rather difficult at present.

Dipped Adcluster Model

For surface-molecule interacting systems in which electron transfer between surface and admolecule is important, the CM and the ECM are insufficient as far as the cluster size is not large enough. However, there are many cases in which the electron transfer seems to be very important; oxygen and halogen chemisorptions on a metal surface, the roles of alkali metals and halogens as promoters, and the activity of electropositive metals for dissociative adsorptions of CO, N_2, and so forth. The dipped adcluster model (DAM) [4,5] has been proposed for dealing with such systems. Since this model has been published 5 years ago, the accounts are given only briefly for being pertinent to the following applications.

Figure 6 illustrates the concept of the DAM. The adcluster is a combined system of an admolecule and a cluster and it is dipped onto the electron "bath" of the bulk metal. Then, electron and spin exchanges occur between the adcluster and the solid until the equilibrium is established for the exchange. The equilibrium would be established when the chemical potential of the adcluster becomes equal to the chemical potential of the surface,

$$-\frac{\partial E(n)}{\partial n} = \mu \tag{9}$$

or more generally when the following condition is satisfied,

$$\min(E(n)) \text{ in the range } -\frac{\partial E(n)}{\partial n} \geq \mu \tag{10}$$

where $E(n)$ is the energy of the adcluster as a function of n, the number of electrons transferred into the adcluster and μ the chemical potential of the surface. We note that n may be a noninteger since we are dealing with a partial system. In this model, the cluster atoms need not to supply all the electrons transferred into the adcluster: some are supplied from the electron bath of the solid.

Previously, we explained several general behaviors of the $E(n)$ curves and their implications [4]. Depending on the shape of the $E(n)$ curve, either a partial electron

transfer or one or two (integral) electron transfer may occur. We have proposed the molecular orbital model of the dipped adcluster [4]. We have assumed that only the active MO of the adcluster, like HOMO, LUMO, or SOMO, is partially filled in the electron-transfer process. There are two extreme ways of spin occupation in the active MO. One is the highest spin coupling in which α spin electron is first occupied and after the occupation reaches unity, the β spin electron is then added. The other is the paired spin coupling in which equal number of α and β spin electrons occupy the active MO. The former model is locally paramagnetic and the latter always diamagnetic. Energetically, the former is more stable than the latter.

When an electron is transferred from a surface to an admolecule, the electrostatic interaction between them would become important. For a metal surface, the so-called image force would occur and its inclusion was described in Ref. [5]. For a semiconductor surface, the interaction should be more localized and such treatment was described in Ref. [4].

Potential Curves of Dioxygen Anion Species

In the next section, we study O_2 chemisorption on an Ag surface. On a metal surface, oxygen is adsorbed in molecular and dissociative states and they are negatively charged as superoxide, O_2^-, peroxide O_2^{2-}, and atomic anions O^- and O^{2-}. Here, we investigate the bondings and the potential curves of the dioxygen anion species O_2^- and O_2^{2-} in their isolated free states for giving a comparative basis [12].

The gaussian basis is the Huzinaga–Dunning (9s5p)/[4s2p] set [13] plus diffuse s,p functions ($\alpha = 0.059$) and polarization d functions ($\alpha = 0.30$), which gives the electron affinity of oxygen atom as 0.97 eV, after electron correlation is included, in comparison with the experimental value of 1.31 eV.

We calculate the potential curves of O_2^- and O_2^{2-} by the SAC (symmetry adapted cluster)/SAC–CI method [14–16]: O_2^{2-} is calculated by the SAC method, since it is a closed-shell molecule, and O_2^- is calculated by the SAC–CI method as a cation produced from O_2^{2-}. Figure 7 shows the result. Table II gives a summary of the spectroscopic constants. The superoxide O_2^- is a stable molecule with the dissociation

TABLE II. The bond length R_e, vibrational frequency ω_e, dissociation energy D_e, electron affinity EA, and gross charge of the O_2^- and O_2^{2-} molecules in a gas phase and of the superoxide O_2^- and peroxide O_2^{2-} species on a silver surface.

Species	Method	R_e (Å)	ω_e (cm^{-1})	D_0 (eV)	EA (eV)	Gross charge (per O_2)
O_2^-	SAC–CI	1.44	1010	4.00	−6.24	−1
	exptl.	1.35	1090	4.09		−1
O_2^{2-}	SAC	1.67	545	−2.94 (0.70)[a]		−2
O_2^- on Ag surface	SAC–CI, DAM	1.47	974, 1055			−0.54, −0.65
	exptl.		1053			
O_2^{2-} on Ag surface	SAC–CI, DAM	1.66	689			−1.4
	exptl.	1.47 ± 0.05	628, ca. 697			

[a] Hump height.

energy of 4.00 eV (experimental value is 4.09 eV). The calculated equilibrium length and the vibrational frequency are 1.44 Å and 1010 cm^{-1} in reasonable agreement with the experimental values 1.35 Å and 1090 cm^{-1}. On the other hand, the peroxide O_2^{2-} is only a transient species though it has a minimum at $R_{O-O} = 1.67$ Å with the hump height of 0.703 eV. The repulsive tail in the longer region is shown to be entirely due to the electrostatic repulsion between the negatively charged oxygen atoms [12].

Dipped Adcluster Model Applied to O_2 Chemisorption on an Ag Surface

O_2 chemisorption on an Ag surface is of interest to many investigators because this system shows very efficient catalytic activity for partial oxydation of ethylene giving ethylene oxide [17]. Several theoretical studies have been published using CM with inclusion of electron correlations [18–20]. Though they could describe the geometry and the vibrational frequency of the adsorbed O_2 in good agreement with experiment, they failed to reproduce the adsorption energy and the dissociatively adsorbed states. Actually, most calculated adsorption energies were negative.

We think that the reason of the failure lies in its model, that is, the CM. The effect of the electron transfer from the bulk metal to the adcluster and the electrostatic image force interaction between O_2 and an Ag surface, which are included in the DAM but not in the CM, are expected to be important for this system.

We first take Ag_2O_2 as an adcluster and consider side-on bridge form interaction. The Ag–Ag distance is fixed at 2.8894 Å, which is the equilibrium distance in the solid. The gaussian basis set for Ag is (3s3p4d)/[3s3p2d] set with the effective core potential for Kr core [21]. For oxygen, the basis set is the same as that used in the preceding section.

Before doing electron correlation calculations, we have applied the molecular orbital model of the dipped adcluster using the highest spin coupling model. The resultant $E(n)$ curve has shown the occurrence of one electron transfer from the bulk Ag solid to the adcluster. We have therefore performed electron-correlation calculations for the Ag_2O_2 anion as the adcluster using the SAC/SAC–CI method [14–16], which is applicable to the ground and excited states of both neutral and electron transferred states. We have included all the valence electrons, together with the d-electrons of Ag, into electron correlation calculations.

Figure 8 is a display of the potential curves for the process of O_2 approach onto Ag_2 dipped onto the metal bulk. The broken lines are the results without the electron transfer ($n = 0$) and the solid one with the electron transfer ($n = 1$). Without the electron transfer, the potential curve, denoted by $^3B_2$ ($n = 0$), is repulsive so that the chemisorption does not occur. Another broken line, denoted by $^3A_2$ ($n = 0$), corresponds to the electron transferred state within the adcluster from Ag_2 to O_2. Though this state is attractive, the minimum is less stable than the separated system which is $^3B_2$. Though these curves include the image force corrections, they essentially correspond to the CM calculations and do not explain the occurrence of the O_2 chemisorption. On the other hand, the potential given by the solid line, which is for the electron transferred state of the DAM, stabilizes as O_2 approaches Ag_2. The asterisk at about 2.5 Å is obtained by the optimization of the O–O distance

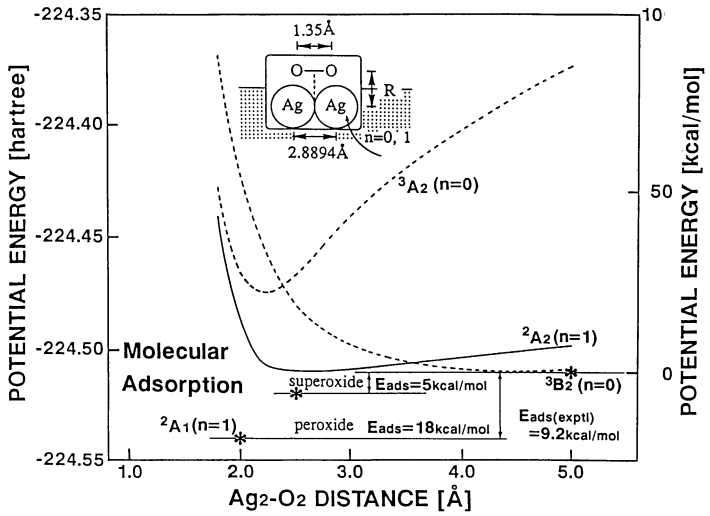

Figure 8. Potential energy curves for the approach of O_2 onto Ag_2 in the Ag_2O_2 adcluster. *n* denotes the number of electrons transferred from the bulk metal to the adcluster.

and corresponds to the superoxide state. The calculated adsorption energy is 3 kcal/mol. Near 2.0 Å, there are another minimum corresponding to the peroxide state and the adsorption energy is 16 kcal/mol. The experimental molecular adsorption energy is 9.2 kcal/mol [22]. Thus, the adsorption energy calculated by the DAM is positive and agrees well with the experimental value.

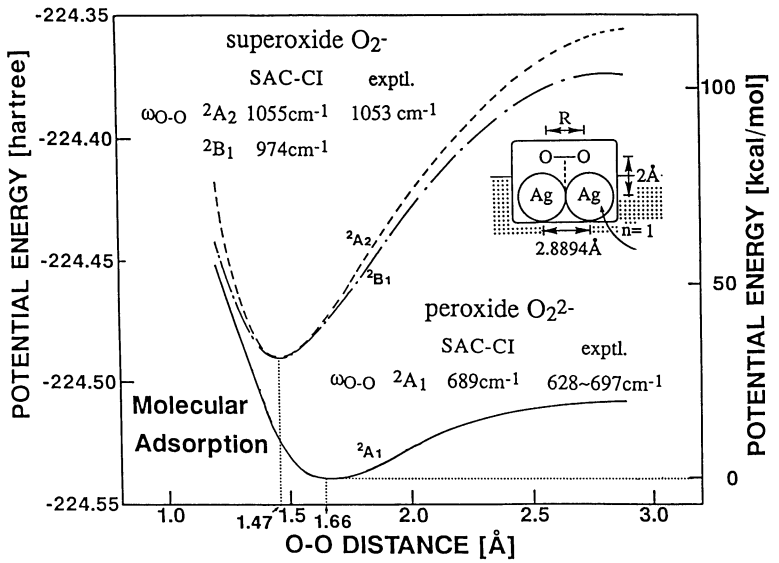

Figure 9. Potential energy curves for the O—O stretching in the Ag_2O_2 adcluster.

We next study the potential curve for the O–O stretching on a silver surface using again the Ag_2O_2 adcluster. Figure 9 and Table II show the results. The lowest solid curve is for the peroxide and the upper two curves for the superoxides. As shown in the figure, the calculated vibrational frequencies agree quite well with the experimental values [23], showing that the molecular adsorption states expressed by the DAM correspond well to the actual systems observed experimentally. The equilibrium O–O distance is 1.47 Å for the superoxide and 1.66 Å for the peroxide. In comparison with the spectroscopic values of O_2^- and O_2^{2-} in their free states, the peroxide state on an Ag surface has very similar vibrational frequency, through the charge on O_2 is only −0.54 ca.−0.65. The peroxide on an Ag surface has a larger vibrational frequency than that in a gas phase, because the former is a stable species in contrast to the transient nature of the latter.

In Figure 9, a point of dissapointment at a first glance is a lack of the dissociatively adsorbed state. Up to the O–O distance of 2.8874 Å, which is the distance of the Ag lattice, the potential monotonously increases. However, at this distance, we found that the gross charge on oxygen is −0.72, so that the electrostatic repulsion between the two oxygens amounts as large as 60 kcal/mol. Therefore, we expect that if we further elongate the O–O distance, we should get a stabilization which might lead to the second minimum corresponding to the dissociatively adsorbed state. For this purpose, we undertake the DAM calculation for O_2 on the linear Ag_4.

The results for the Ag_4–O_2 adcluster are displayed in Figure 10. We certainly get two different potential minima. The minima at around 1.5 to 1.7 Å correspond to the molecular adsorption states (superoxide and peroxide) and another minimum at about 6 to 7 Å corresponds to the dissociatively adsorbed state. The dissociative state is obtained from the peroxide molecular adsorption state. After the optimization of the O–O and Ag–O distances, the dissociated state is calculated at the asterisk

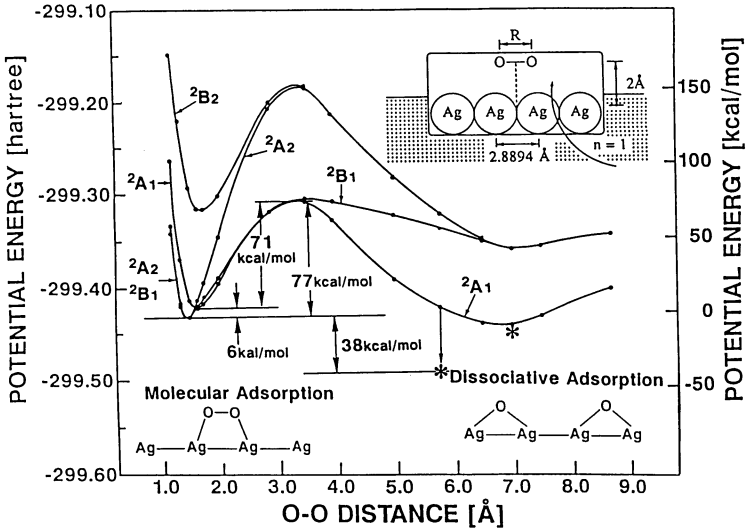

Figure 10. Potential energy vs. the O–O distance in the Ag_4O_2 adcluster.

at the O–O distance of 5.78 Å. The dissociative state is calculated to be more stable than the molecular adsorption state by about 40 kcal/mol: the corresponding experimental value is 31 to 33 kcal/mol [22].

Thus, using the DAM and the SAC–CI method, we could successfully describe the O_2 chemisorption on an Ag surface. The inclusions of the electron transfer from the bulk Ag metal to the adcluster and the electrostatic image force correction described by the DAM, and the electron correlations for several lower surface states described by the SAC–CI method are the reason of the success of the present study.

Acknowledgment

The author thanks Dr. H. Nakai and Mr. Y. Fukunishi for active collaborations. The calculations included in this review are carried out with the use of the computers at the computer centers of the Institute for Molecular Science and at Kyoto University. Parts of these studies were supported by the Grant-in-Aids for Scientific Research from the Ministry of Education, Science, and Culture of Japan.

Bibliography

[1] T. B. Grimley and C. Pisani, J. Phys. C**7**, 2831 (1974); T. B. Grimley and E. E. Mola, *ibid.* C**9**, 3437 (1976).
[2] C. Pisani, Phys. Rev. B**17**, 3143 (1978).
[3] W. Ravenek and F. M. M. Geurts, J. Chem. Phys. **84**, 1613 (1986).
[4] H. Nakatsuji, J. Chem. Phys. **87**, 4995 (1987).
[5] H. Nakatsuji, H. Nakai, and Y. Fukunishi, J. Chem. Phys. **95**, 640 (1991).
[6] Y. Fukunishi and H. Nakatsuji, J. Chem. Phys. (in press).
[7] H. Nakatsuji and H. Nakai, Chem. Phys. Lett. **174**, 283 (1990).
[8] H. Nakatsuji and H. Nakai, Can. J. Chem. (in press).
[9] H. Nakatsuji and H. Nakai, J. Chem. Phys. (in press).
[10] H. Nakai, Y. Ohmori, and H. Nakatsuji, J. Chem. Phys. **95**, 8287 (1991).
[11] H. Nakatsuji, H. Nakai, and Y. Ohmori (submitted for publication).
[12] H. Nakatsuji and H. Nakai, Chem. Phys. Lett. (in press).
[13] S. Huzinaga, J. Chem. Phys. **42**, 1293 (1965); T. H. Dunning, Jr., *ibid.* **53**, 2823 (1970).
[14] H. Nakatsuji, Chem. Phys. Lett. **67**, 329 (1978).
[15] H. Nakatsuji, Theor. Chim. Acta **71**, 201 (1987).
[16] H. Nakatsuji, Acta Chimica Hungarica (in press).
[17] A. Ayame and H. Kanoh, Shokubai **20**, 381 (1978) (in Japanese).
[18] A. Selmani, J. Andzelm, and D. Salahub, Int. J. Quantum Chem. **29**, 829 (1986).
[19] T. H. Upton, P. Stevens, and P. J. Madix, J. Chem. Phys. **88**, 3988 (1988).
[20] E. A. Carter and W. A. Goddard III, Surf. Sci. **209**, 243 (1989).
[21] P. J. Hay and W. R. Wadt, J. Chem. Phys. **82**, 270 (1985).
[22] C. T. Campbell, Surf. Sci. **157**, 43 (1985).
[23] C. Pettenkofer, I. Pockrand, and A. Otto, Surf. Sci. **135**, 52 (1983); C. Pettenkofer, J. Eickmans, U. Erturk, and A. Otto, *ibid.* **151**, 9 (1985).

Received April 20, 1992